Bioorganic & Medicinal Chemistry Letters 22 (2012) 4296–4302

Contents lists available at SciVerse ScienceDirect

Bioorganic & Medicinal Chemistry Letters

journal homepage: www.elsevier.com/locate/bmcl

Potent and selective inhibitors of PI3Kδ: Obtaining isoform selectivity from the affinity pocket and tryptophan shelf

Daniel P. Sutherlin [a,*], Stewart Baker [b], Angelina Bisconte [a], Paul M. Blaney [c], Anthony Brown [b], Bryan K. Chan [a], David Chantry [a], Georgette Castanedo [a], Paul DePledge [b], Paul Goldsmith [b], David M. Goldstein [d], Timothy Hancox [b], Jasmit Kaur [b], David Knowles [b], Rama Kondru [d], John Lesnick [a], Matthew C. Lucas [d], Cristina Lewis [a], Jeremy Murray [a], Alan J. Nadin [c], Jim Nonomiya [a], Jodie Pang [a], Neil Pegg [b], Steve Price [c], Karin Reif [a], Brian S. Safina [a], Laurent Salphati [a], Steven Staben [a], Eileen M. Seward [c], Stephen Shuttleworth [b], Sukhjit Sohal [b], Zachary K. Sweeney [a], Mark Ultsch [a], Bohdan Waszkowycz [c], Binqing Wei [a]

[a] Genentech, Inc., 1 DNA Way, South San Francisco, CA 94080, USA
[b] Piramed Pharma, 957 Buckingham Avenue, Slough, Berks SL1 4NL, United Kingdom
[c] Argenta Discovery, 8/9 Spire Green Centre, Flex Meadow, Harlow CM19 5TR, United Kingdom
[d] Roche Research Center, 340 Kingsland Street, Nutley, NJ 07110, USA

ARTICLE INFO

Article history:
Received 16 February 2012
Revised 3 May 2012
Accepted 8 May 2012
Available online 17 May 2012

Keywords:
PI3K delta inhibitor
PI3K Isoform selectivity
B-cell inhibition
Rhumatoid arthritis

ABSTRACT

A potent inhibitor of PI3Kδ that is ⩾200 fold selective for the remaining three Class I PI3K isoforms and additional kinases is described. The hypothesis for selectivity is illustrated through structure activity relationships and crystal structures of compounds bound to a K802T mutant of PI3Kγ. Pharmacokinetic data in rats and mice support the use of **3** as a useful tool compound to use for in vivo studies.

The phosphatidylinositol 3-kinase delta isoform (PI3Kδ) has been identified as a potential drug target for diseases that are related to immune cell function. Two clear examples of these diseases include B-cell mediated hematological malignancies such as chronic lymphoid leukemia (CLL) where, **2** (Cal-101, Fig. 1), a selective PI3Kδ inhibitor, has resulted in positive clinical responses,[1–3] and the auto-immune disease rheumatoid arthritis (RA).[4] In our efforts to discover a potent and selective PI3Kδ drug candidate, a tool molecule was identified that combines the potency, isoform selectivity, and pharmacokinetic (PK) profile required to explore exclusively the biology of PI3Kδ inhibition in vivo. Furthermore, selectivity for the delta isoform relative to the other Class I PI3Ks was obtained through molecular interactions that have not been exploited by previous inhibitors.

PI3Ks are lipid kinases that convert the second messenger phosphatidylinositol (4,5)-bisphosphate (PIP2) to phosphatidylinositol (3,4,5)-trisphosphate (PIP3), which results in the activation of AKT and other downstream signaling events. The Class I PI3K family is composed of four highly homologous isoforms, PI3Kα, β, δ, and γ which are activated by receptor tyrosine kinases (in the case of isoforms α, β, δ) or GPCRs (for PI3Kγ).[5,6] Whereas PI3Kα and β are ubiquitously expressed, PI3Kδ and γ are expressed almost exclusively in leukocytes, providing the opportunity to specifically target hematologic and inflammatory diseases with compounds that are selective for the latter isoforms.[7]

In B-cells, PI3Kδ functions downstream of the B-cell receptor which is important for antigen recognition and B-cell proliferation.[8,9] PI3Kδ knockout (KO) or kinase dead (KD) knock in mice have reduced numbers of progenitor B-cells that are less proliferative in response to stimuli.[10,11] Additionally, in vitro inhibition of PI3Kδ with the selective tool compound **1** (IC87114) reproduces the observed phenotypes of B-cells isolated from KO or KD mice.[12] PI3Kδ is also downstream of a number of other receptors found in a variety of leukocytes that are important to immune cell function. These include the T-cell receptor in T-cells, the FceRI and c-kit in

* Corresponding author. Tel.: +1 650 225 3171.
E-mail address: sutherd1@gene.com (D.P. Sutherlin).

0960-894X/$ - see front matter © 2012 Elsevier Ltd. All rights reserved.
http://dx.doi.org/10.1016/j.bmcl.2012.05.027

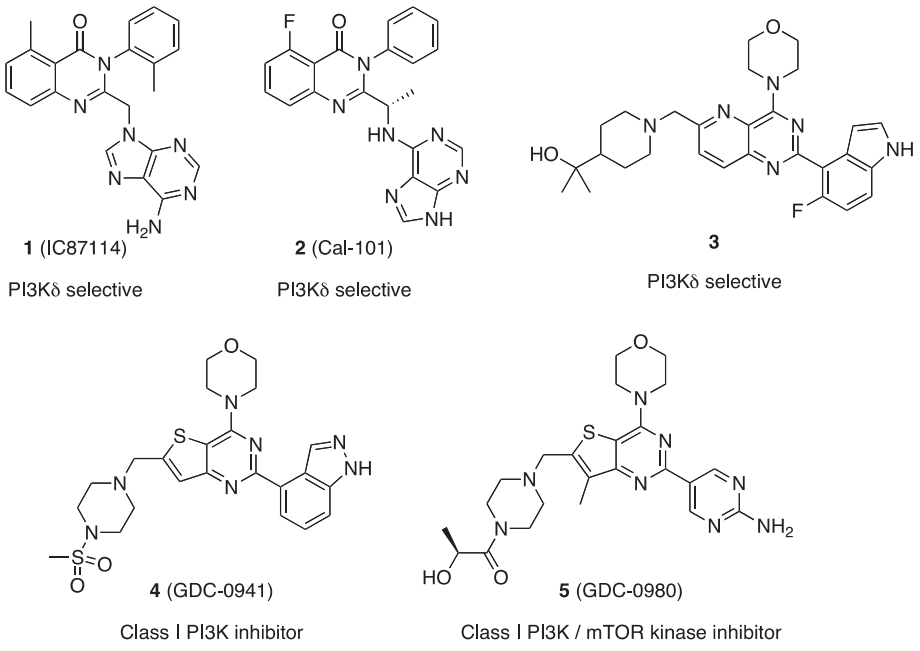

Figure 1. PI3Kδ inhibitors from isoform selective and isoform non-selective scaffolds.

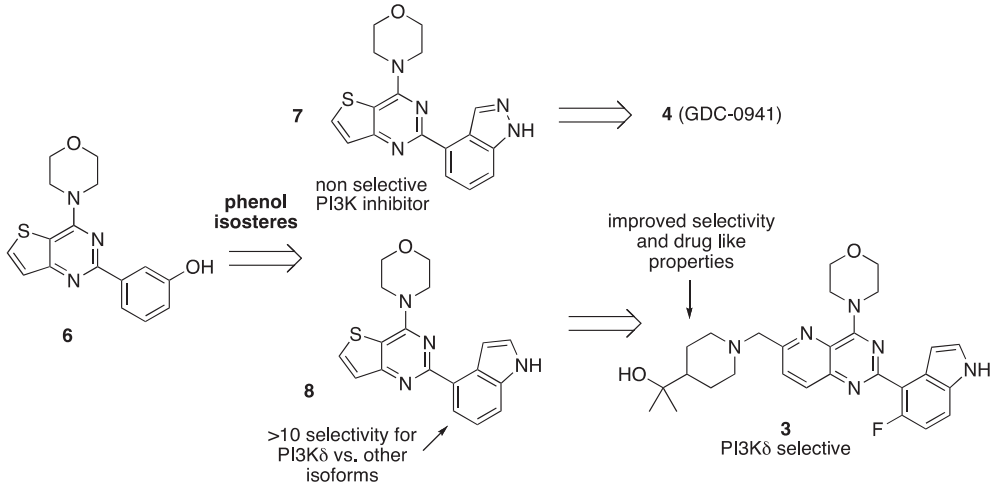

Figure 2. Discovery of **3** starting from phenol **6**.

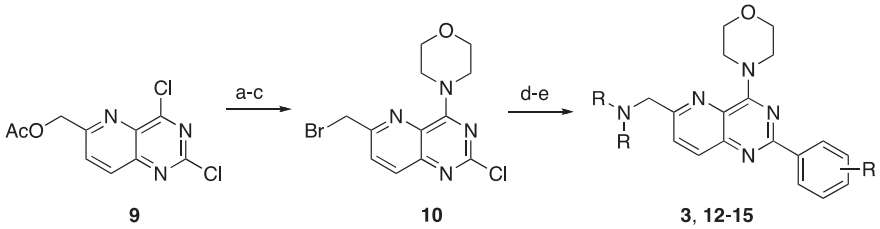

Scheme 1. Synthesis of **3** and related analogs. Reagents and conditions: (a) morpholine, EtOH, 2 h, 96%; (b) LiOH, THF, 2 h, 100%; (c) PPh_3, NBS, CH_2Cl_2, 0 °C, 0.5 h, 87%; (d) R_2NH, iPr_2EtN, MeOH, THF, rt, 1.5 h, 60–100%; (e) boronic acid/ester, $Pd(PPh_3)_2Cl_2$, 1 M Na_2CO_3, CH_3CN, microwave, 140 °C, 0.5 h, 22–54%.

mast cells, and as well as chemokine receptors in B-cells[13] and neutrophils.[14] Many of these same cell types have been linked to the pathogenesis of inflammatory diseases and hematologic malignancies, making PI3Kδ an attractive target for a wide variety of diseases including rheumatoid arthritis, asthma and leukemias.[15]

Several classes of PI3Kδ isoform selective inhibitors have been described in the literature along with a structural hypothesis for their selectivity.[16] The delta selective compounds **1** (IC87114) and **2** (Fig. 1) adopt a 'propeller shape' and induce a conformational change in the protein that opens a specificity pocket between

Table 1
PI3Kδ selective compound **3** and SAR related to isoform selectivity

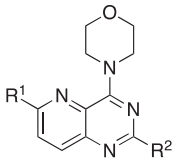

Compound	R^1	R^2	IC_{50} (nM)	Fold selectivity			IC_{50} (nM)
			p110δ	α/δ	β/δ	γ/δ	(Ri-1) pAKT
3	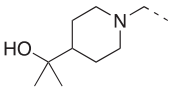	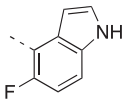	3.8	340	200	410	40
12	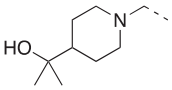	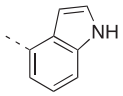	2.8	370	210	610	55
13	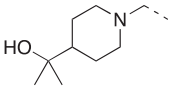	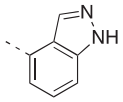	6.3	22	78	260	480
14	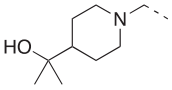	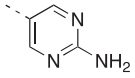	2.6	5.4	73	43	145
15	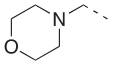	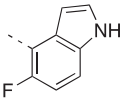	12	58	13	120	67
16		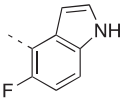	27	14	3.7	38	145

a tryptophan (Trp812, gamma numbering) and a methionine (Met804).[17] We have identified **3**, a potent inhibitor of PI3Kδ that is 200–400 fold selective for all three remaining Class I PI3K isoforms yet resembles the same compound class of inhibitors represented by the Class I PI3K inhibitor **4** (GDC-0941)[18] and Class I PI3K/mTOR kinase inhibitor **5** (GDC-0980)[19] that inhibit all four PI3K isoforms and are currently in oncology trials. Based on this selectivity and PK profile, **3** can achieve plasma levels in rodents that can exceed an IC_{90} measure of whole blood B-cell activation, driven by PI3Kδ inhibition, without significantly inhibiting other PI3K isoforms.

The discovery of selective compound **3** was inspired by early work where isosteres of phenol **6** were successfully used to improve oral bioavailability in this simple scaffold that possessed good potency for all PI3K isoforms and favorable biopharmaceutical properties.[18] Where, indazole **7** eventually led to the discovery of **4**, indole **8** was found to impart a significant amount of selectivity for PI3Kδ relative to the other three isoforms (Fig. 2). The addition of a basic amine, extended to solvent, improved overall potency, solubility, and ADME properties of the scaffold. This change also increased isoform selectivity especially when hydrophobic groups were included. These efforts culminated in a number of potent and selective PI3Kδ inhibitors of which **3** is a representative. Herein we use SAR and co-crystal structures of this optimized compound to rationalize the contributions that these functionalities make to isoform selectivity.

Compound **3** and related analogs were prepared according to Scheme 1 or as previously reported.[19–21] Biochemical potencies were measured using a fluorescence polarization assay that monitored the conversion of PIP2–PIP3. Cell based potencies were generated by monitoring the up-regulation of the cell surface B-cell marker CD69 in whole blood[22] or a downstream signaling product of PI3K, pAKT, in a PI3Kδ-dependent B-cell cancer cell line in the presence of human serum. These assays demonstrate that **3** is highly potent for PI3Kδ with an IC_{50} of 3.8 nM in the biochemical assay, a 41 nM IC_{50} in the human whole blood assay, and an IC_{50} of 40 nM in the serum-shifted B-cell pAKT assay. The B-cell pAKT assay was used routinely for assessment of SAR due to the excellent concordance between this assay and the B-cell CD69 whole blood assay. Compound **3** was also >200 fold selective for PI3Kδ over the other three Class I PI3K isoforms (Table 1) and extremely selective relative to 239 kinases tested in Invitrogen's SelectScreen service (0/239 kinases showing >50% inhibition when tested at 1 μM; mTOR, DNA-PK, VPS34, and PI4Kα & β were inhibited at 10% or less when tested at 1 μM; PIKC2A & B were inhibited at 11% and 42%, respectively, at this same concentration and showed less than 10% inhibition when tested at 0.1 μM; the PIKK family kinases ATM and ATR were not assessed.).

Compounds in Table 1 demonstrate the trends in isoform selectivity that were observed across a large number of analogs. The des-fluoro analog **12**, illustrates that this halogen does not play a critical role in the selectivity of these compounds (this substitution was used to block potential sites of oxidation). However, the indazole or aminopyrimidine analogs **13** and **14** that are related to the non-selective Class I PI3K inhibitors **4** and **5**, have eroded isoform selectivity, especially for alpha, while maintaining delta potency. On the opposite side of the molecule, truncation of the R1 substituted piperizine to a less extended morpholine **15** and hydroxymethyl **16** primarily resulted in a loss of PI3Kδ potency and, consequently, isoform selectivity especially for the alpha and beta isoforms. Cellular B-cell pAKT potencies determined with serum added are listed and are a result of a combination of enzyme potency and amount of unbound compound.

The identity of the core does not have a dramatic influence on isoform selectivity or potency when using identical substituents

Table 2
SAR for core changes to compound **3**

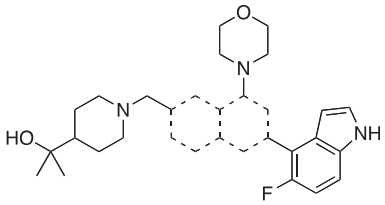

Compound	Core	IC_{50} (nM)	Fold selectivity		
		p110δ	α/δ	β/δ	γ/δ
3	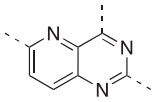	3.8	340	200	410
17	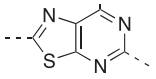	0.6	220	200	1400
18	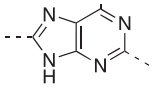	1.9	330	140	1500
19	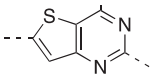	4.0	170	110	910

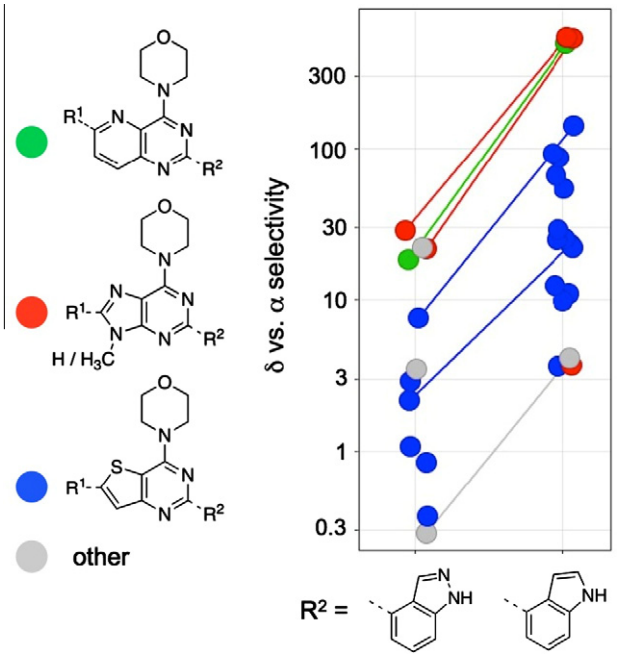

Figure 3. PI3Kδ selectivity versus PI3Kα compared for different cores and R groups. Selectivity for PI3Kδ versus PI3Kα for individual molecules are indicated by a colored spot on the graph. Blue dots represent thienopyrimidine cores; red, purine cores; green, pyridopyrimidine cores; and gray, other pyrimidine based cores. The compounds are then segregated by the identity of the substituent in the activity pocket indicated by R^2, an indazole or an indole. Matched pairs, compounds that are identical in every respect except for the identity of the R^2 group, are linked on the graph by a line.

(Table 2). A minor but consistent erosion of selectivity for PI3Kα and PI3Kβ relative to PI3Kδ was observed as the distance between the piperidine substituent and the morpholine increased. Minor perturbations in structure resulted in small, but significant, alterations in the angle that the piperidine substituent projected from the core.

The SAR trends described in Tables 1 and 2 hold up well when looking at a larger number of analogs. Figure 3 highlights a comparison of compounds with a variety of R^1 groups in the solvent exposed region, an R^2 unsubstituted indazole or indole, and the three cores shown in Table 2. This analysis demonstrates that, on average, compounds that contain an indole are more selective for PI3Kδ versus PI3Kα than those compounds containing an indazole. Furthermore, when matched pairs[23] of identical compounds, differing only by an indazole or indole, are compared (dots connected by solid lines), compounds are consistently ~20 fold more selective with the indole regardless of the identity of the core or R^1 substituent.

In order to illustrate the structural hypothesis that we believe explains selectivity for PI3Kδ versus the other three Class I isoforms we sought to obtain a co-crystal structure of **3** bound to PI3Kγ. Although, PI3Kδ structures have been reported, extensive structural work in PI3Kγ by several groups has been successfully used to describe binding modes and explain aspects of isoform selectivity of compounds like **1**, **4**, and **5**. The affinity pocket where the indole of **3** is expected to bind (based on co-crystal structures of **4**) is highly homologous across all four isoforms of PI3K, a somewhat surprising observation given the degree of selectivity that can be obtained for PI3Kδ in this region of the protein. In contrast to this structural similarity, there are differences in residues that surround the solvent exposed entrance to the active site. For our molecules, the most relevant sequence difference was a threonine found at position 802 in PI3Kδ (PI3Kγ numbering) that is substituted by a larger, charged lysine or arginine in the other three Class I isoforms (Fig. 4). These residues are located directly above conserved Trp812 and are in proximity to where R1 substituents were known to bind. The structural impact of this sequence difference is the formation of a hydrophobic dimple or a 'tryptophan shelf' in PI3Kδ that was thought to play a role in the selectivity for our class of inhibitors. This change has also been implicated in the selectivity of a previously reported scaffold class, exemplified by the compound AS15.[17] To address this difference we prepared and obtained crystal structures of several compounds bound to a (K802T) mutant of PI3Kγ that we hoped would replicate the shape of the PI3Kδ binding site.

As expected, **3** bound to (K802T) PI3Kγ in a manner similar to previously described Class I PI3K inhibitors **4** and **5**.[24] The morpholine makes a critical interaction to the hinge and the core projects the indole into the affinity pocket where it makes a favorable H-bond to Asp841 (Fig. 5A). In the solvent exposed region of the binding site, the 4-substituted piperidine occupies the tryptophan shelf made available via the K802T mutation in PI3Kγ (Fig. 5B). This structural change allows the methyl groups of the tertiary alcohol to make hydrophobic contacts with the face of tryptophan that is occluded in other PI3Kα and PI3Kγ structures. This direct interaction with the face of the tryptophan is different from interactions made by compound classes like those represented by **1**. In contrast, **1** has been shown to induce the formation of a 'specificity pocket' and allows the central quinazolone ring to insert between the tryptophan and methionine, two residues that are typically adjacent to one another (Fig. 5C). In this unique conformation of the protein, the planar quinazolone ring makes favorable interactions with the edge of the tryptophan and van der Waals interactions with the methionine and an isoleucine in the back of the newly formed pocket. This single modification did not significantly alter the biochemical potency of **1** or **3** when compared to wild type PI3Kγ and suggests that additional changes to the non-conserved amino acids surrounding Trp812 may also be necessary to recapitulate the binding affinity observed in the PI3Kδ isoform. In particular there are four residues that are <6 Å away from Trp812 that are different in both isoforms; Glu814, Lys800, Ile881, and Gln784 in PI3Kγ

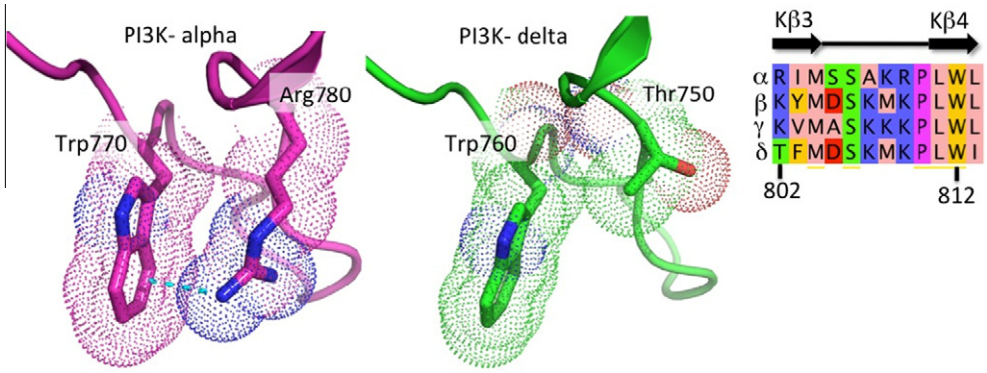

Figure 4. Comparison of the tryptophan region for crystal structures of PI3Kδ and PI3Kα. The solvent accessible surface in the vicinity of Trp812 (gamma numbering) for PI3Kα in magenta (PDB code 3HHM) and PI3Kδ is shown in green (PDB code 2WXP). A sequence alignment for all four isoforms between residues 802 and 813 (gamma numbering) highlights the conserved tryptophan at position 812 and the unique threonine 802 in delta.

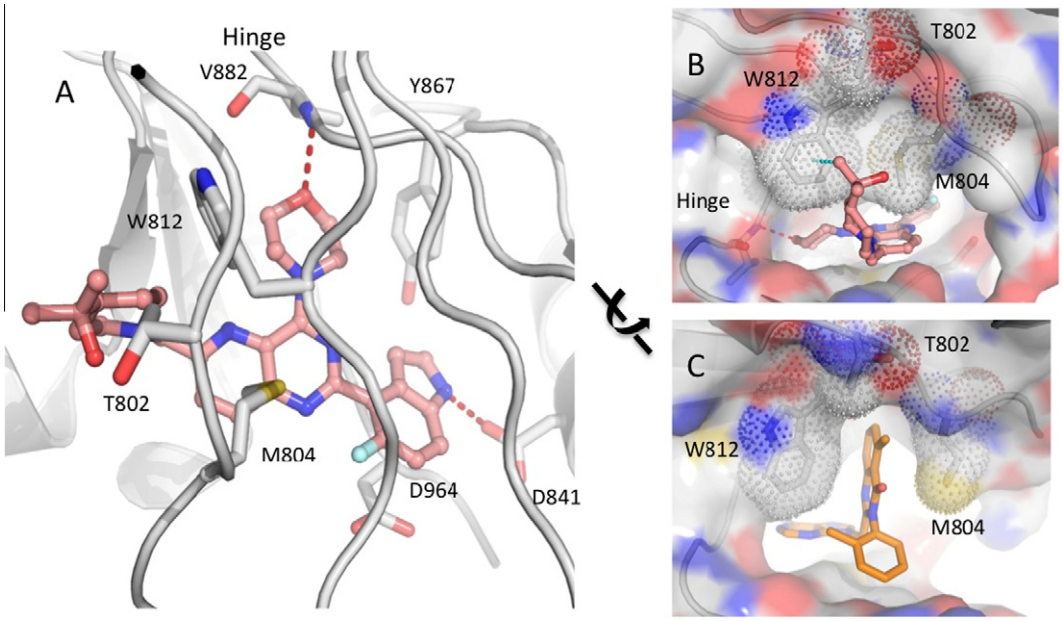

Figure 5. (A–C) Co-crystal structure of **3** bound to (K802T) PI3Kγ and **1** bound to PI3Kδ (PDB 2X38). (A) The morpholine of **3** (pink) makes a 2.6 Å hydrogen-bond to the hinge region of the kinase and the NH of the indole makes a 2.8 Å hydrogen-bond to Asp841. Met804 sits directly above the pyridyl ring of the core. (B) As viewed from solvent, compound **3** emerges from the active site. The dimethyl alcohol on the piperidine interacts with the tryptophan shelf formed by W812 and T802. (C) Compound **1** (orange) bound to PI3Kδ and showing the qinazolone of **1** sandwiched between the tryptophan and methionine.

align with Gln784, Met762, Val827, and Lue829 in PI3Kδ (not shown).

In contrast to the appealing hypothesis of the tryptophan shelf's contribution to isoform selectivity, a structural explanation for the selectivity obtained in the affinity pocket by the indole is more elusive. However, several co-crystal structures of compounds including **4–5** in PI3Kγ[18,19] as well as **3**, **13** and **14** bound to (K802T) PI3Kγ (Fig. 6) suggest that selective indole-containing molecules interact with the conserved Tyr867 through an alternative hydrogen-bond network to that observed with the less-selective indazoles or aminopyrimidines.[25] The structure of **3** bound to (K802T) PI3Kγ shows the indole ring C–H being directed at the oxygen of Tyr867 and places the indole carbon and tyrosine oxygen 3.1 Å from one another (Fig. 6A). The phenol OH of this Tyr867 then makes a 2.6 Å hydrogen-bond to a backbone carbonyl of His962 and thus engages the conserved HxD motif[26] that resides in the DFG loop. This network of interactions is conserved when looking over six additional structures of indole-containing inhibitors bound to PI3Kγ (indole C to tyrosine O average distance was 3.0 ± 0.23 Å and the tyrosine OH to histidine CO distance was 3.3 ± 0.11 Å).

Structures of compounds that contain the isosteric indazole where an H-bond accepting nitrogen replaces the indole CH suggests an opposite hydrogen-bonding scenario. As examples, the previously described structure of **4** in PI3Kγ18 and **13** in (K802T) PI3Kγ show likely hydrogen-bonds from Tyr867 to the indazole nitrogen with an 2.6 and 2.9 Å distance, respectively, (**13** shown in Fig. 6B). This interaction is expected to result in an unfavorable interaction between the oxygen lone pairs of the tyrosine hydroxyl and the backbone carbonyl of the histidine, and increases the distance between these two oxygens to 4.0 and 3.8 Å in the structures of **4** and **13**, respectively. Furthermore, the non-selective aminopyrimidines exemplified by **5**[19] and **14** also show an increased distance between the side chain and backbone oxygens (Fig. 6C). This oxygen to oxygen distance is measured at 3.9 Å for **5**, 3.6 Å for **14**, and an average of 4.3 Å when looking at structures of additional aminopyrimidines bound to PI3Kγ.[27] It is proposed that the tyrosine hydroxyl makes a water mediated H-bond to the aminopyrimidine ring

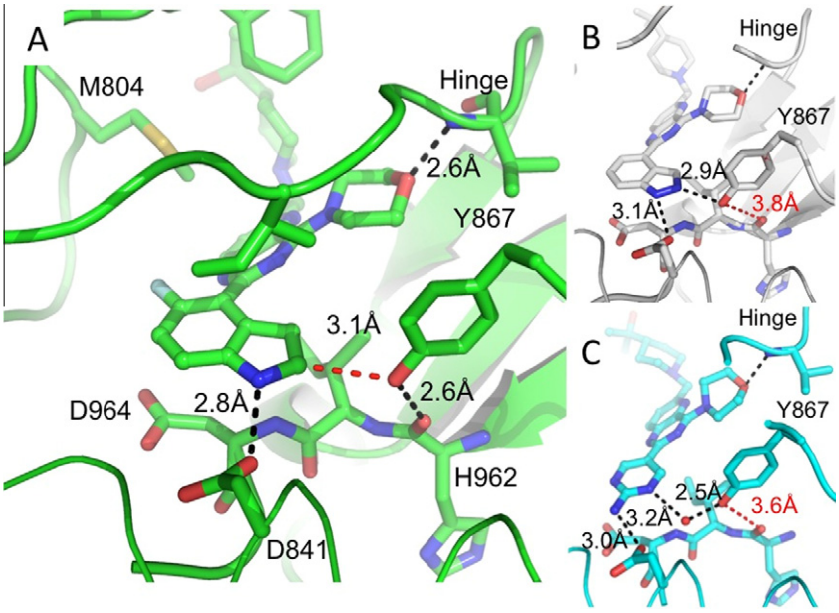

Figure 6. (A–C) Detail of the key interactions in the affinity pocket for selective PI3Kδ inhibitor **3** (green), and Class I PI3K inhibitors **13** (gray), and **14** (turquois)[a]. Black dashed lines indicate proposed hydrogen-bonds with measurements included. Additional atom–atom distances that have been measured are shown by red dashes.

Table 3
Pharmacokinetic parameters for compound **3**[a]

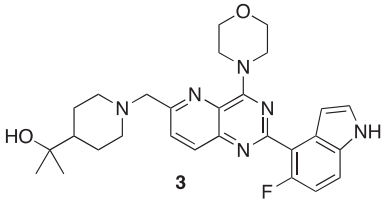

3

Species	In vitro mics. Cl_{hep} (mL/min/kg)	IV (1 mg/kg)		PO				
		In vivo CI (mL/min/kg)	V_{ss} (L/kg)	Dose (mg/kg)	C_{max} (μM)	AUC (μM h)	$T_{1/2}$ (h)	PPB%
Mouse	47	53	4.9	5	0.9	2.5	2.6	88
				20	3.9	13	2.9	–
				40	14	63	5.0	–
Rat	23	59	8.8	5	0.5	2.6	2.6	80
				10	1.2	11	3.8	–
				30	4.7	46	4.8	–

[a] Female mice were dosed IV (intravenously) with **3** in 5% DMSO/5% Cremephor and PO (orally) as an MCT suspension (0.5% methylcellulose/0.2% Tween-80). The IV and 5 mg/kg PO studies were performed in CD-1 mice while the higher dose studies were performed in the Balb/c strain. Male Sprague–Dawley rats were dosed with the same IV and PO formulations as those used for mice. Hepatic clearance was predicted from liver microsome incubations using the 'in vitro $t_{1/2}$ method'.[30]

nitrogen, a hypothesis that is supported by the structure of **14** in (K802T) PI3Kγ. We propose that the PI3Kδ isoform is more able to accommodate this shift in the hydrogen-bonding network within the affinity pocket than in the other isoforms.

The pharmacokinetic properties of **3** were evaluated in mice and rats when dosed IV and orally (Table 3). Hepatic clearances predicted from microsomal incubations matched the in vivo clearance within a twofold margin. Good plasma exposures and reasonable half-lives were observed upon oral dosing, a reflection of high oral bioavailability (80% and 90% at a low dose for mouse and rat, respectively), moderate volume of distribution, and moderate clearance. Plasma exposures and C_{max} levels increased with dose in both mice and rats, important in that inflammatory disease models utilize these two species.[28] The combination of the potency in whole blood, excellent selectivity versus the other three isoforms, and the PK profile of **3** would allow for extensive in vivo target coverage while also minimizing the inhibition of the other isoforms (Fig. 7). Plasma protein binding for **3** ranged from 80–88% in rodents and were consistent with values obtained in human plasma (86%). We considered these factors to be important in the development of a useful tool to explore the biology of PI3Kδ inhibition in vivo.[29]

We have described a potent PI3Kδ inhibitor that is >200 fold selective for the other Class I PI3K isoforms PI3Kα, β and γ. Compound **3** and related molecules achieve this selectivity profile from two regions of the binding site. First, in the affinity pocket, an indole group positions a weak CH hydrogen-bond donor towards a conserved tyrosine that traditionally functions as a hydrogen-bond donor to non-isoform selective inhibitors directly or via bound waters. We suggest that this tyrosine must reorder its hydrogen-bond network in a manner that is accommodated more readily by the PI3Kδ isoform. Secondly, we show that a solvent exposed

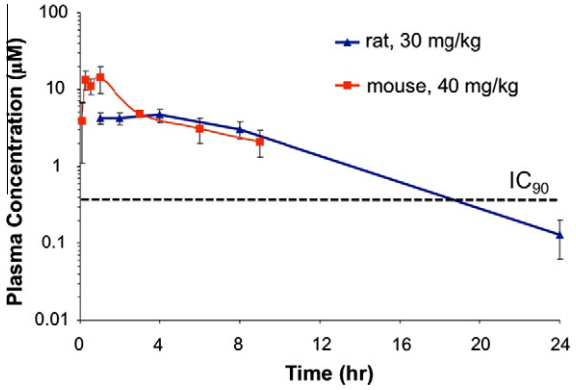

Figure 7. PK curves, showing plasma concentration versus time, for **3** when dosed at 30 and 40 mg/kg in rats and mice, respectively. A projected IC_{90} for B-cell receptor inhibition in human whole blood is placed on the graph to demonstrate the potential utility of these dose levels.

substituted piperidine makes a hydrophobic interaction with a tryptophan shelf that is exposed only in the PI3Kδ isoform. To illustrate this, we have prepared and obtained a crystal structure of **3** and related compounds bound to a PI3Kγ Lys802 to Thr mutant. Furthermore we show that this compound has PK properties in rodents that support its use in animal models of disease where PI3Kδ is thought to play a role.

Acknowledgments

We thank all the scientists at PIramed and Argenta for their pioneering work leading to the discovery and characterization of many selective PI3Kδ inhibitors, invaluable precursors to compound **3**. We thank Mengling Wong, Chris Hamman, Baiwei Lin, and Steve Huhn for compound purification and determination of purity by LCMS, and ^{1}H NMR; Krista K. Bowman, Alberto Estevez, Kyle Mortara, and Jiansheng Wu for technical assistance of protein expression and purification, and Emil Plise for plasma protein binding data and the entire in vivo studies group. We thank Po-Chang Chiang and Amy Sambrone for assistance with formulation of 3 for PK studies.

Supplementary data

Supplementary data associated with this article can be found, in the online version, at http://dx.doi.org/10.1016/j.bmcl.2012.05.027. These data include MOL files and InChiKeys of the most important compounds described in this article.

References and notes

1. Flinn, I. W.; Byrd, J. C.; Furman, R. R.; Brown, J. R.; Lin, T. S.; Bello, C.; Giese, N. A.; Yu, A. S.; Cannon, S. *J. Clin. Oncol.* **2009**, *27*, 3543.
2. Herman, S. E. M.; Gordon, A. L.; Wagner, A. J.; Heerema, N. A.; Zhao, W.; Flynn, J. M.; Jones, J.; Andritsos, L.; Puri, K. D.; Lannutti, B. J.; Giese, N. G.; Zhang, X.; Wei, L.; Byrd, J. C.; Johnson, A. J. *Blood* **2010**, *116*, 2078.
3. Lannutti, B. J.; Meadows, S. A.; Herman, S. E. M.; Kashishian, A.; Steiner, B.; Johnson, A. J.; Byrd, J. C.; Tyner, J. W.; Loriaux, M. M.; Deininger, M.; Druker, B. J.; Puri, K. J.; Ulrich, R. G.; Giese, N. A. *Blood* **2011**, *117*, 591.
4. Rommel, C.; Camps, M.; Ji, H. *Nat. Rev. Immunol.* **2007**, *7*, 191.
5. Cantley, L. C. *Science* **2002**, *296*, 1655.
6. Vanhaesebroeck, B.; Guillermet-Guibert, J.; Graupera, M.; Bilanges, B. *Nat. Rev. Mol. Cell Biol.* **2010**, *11*, 329.
7. Kok, K.; Geering, B.; Vanhaesebroeck, B. *Trends Biochem. Sci.* **2009**, *34*, 115.
8. Okkenhaug, K.; Vanhaesebroeck, B. *Nat. Rev. Immunol.* **2003**, *3*, 317.
9. Okkenhaug, K.; Ali, K.; Vanhaesebroeck, B. *Trends Immunol.* **2007**, *28*, 80.
10. Okkenhaug, K.; Bilancio, A.; Farjot, G.; Priddle, H.; Sancho, S.; Peskett, E.; Pearce, W.; Meek, S. E.; Salpekar, A.; Waterfield, M. D.; Smith, A. J. H.; Vanhaesebroeck, B. *Science* **2002**, *297*, 1031.
11. Clayton, E.; Bardi, G.; Bell, S. E.; Chantry, D.; Downes, C. P.; Gray, A.; Humphries, L. A.; Rawlings, D.; Reynolds, H.; Vigorito, E.; Turner, M. *J. Exp. Med.* **2002**, *196*, 753.
12. Bilancio, A.; Okkenhaug, K.; Camps, M.; Emery, J. L.; Ruckle, T.; Rommel, C.; Vanhaesebroeck, B. *Blood* **2006**, *107*, 642.
13. Reif, K.; Okkenhaug, K.; Sasaki, T.; Penninger, J. M.; Vanhaesebroeck, B.; Cyster, J. G. *J. Immunol.* **2004**, *173*, 2236.
14. Fung-Leung, W.-P. *Cell. Signalling* **2011**, *23*, 603.
15. Marone, R.; Cmiljanovic, V.; Giese, B.; Wymann, M. P. *Biochim. Biophys. Acta* **2008**, *1784*, 159.
16. Ameriks, M. K.; Venable, J. D. *Curr. Top. Med. Chem.* **2009**, *9*, 738.
17. Berndt, A.; Miller, S.; Williams, O.; Le, D. D.; Houseman, B. T.; Pacold, J. I.; Gorrec, F.; Hon, W. C.; Liu, Y.; Rommel, C.; Gaillard, P.; Ruckle, T.; Schwarz, M. K.; Shokat, K. M.; Shaw, J. P.; Williams, R. L. *Nat. Chem. Biol.* **2010**, *6*, 117.
18. Folkes, A. J.; Ahmadi, K.; Alderton, W. K.; Alix, S.; Baker, S. J.; Box, G.; Chuckowree, I. S.; Clarke, P. A.; Depledge, P.; Eccles, S. A.; Friedman, L. S.; Hayes, A.; Hancox, T. C.; Kugendradas, A.; Lensun, L.; Moore, P.; Olivero, A. G.; Pang, J.; Patel, S.; Pergl-Wilson, G. H.; Raynaud, F. I.; Robson, A.; Saghir, N.; Salphati, L.; Sohal, S.; Ultsch, M. H.; Valenti, M.; Wallweber, H. J. A.; Wan, N. C.; Wiesmann, C.; Workman, P.; Zhyvoloup, P.; Zvelebil, M. J.; Shuttleworth, S. J. *J. Med. Chem.* **2008**, *51*, 5522.
19. Sutherlin, D. P.; Bao, L.; Berry, M.; Castanedo, G.; Chuckowree, I.; Dotson, J.; Folks, A.; Friedman, L.; Goldsmith, R.; Gunzner, J.; Heffron, T.; Lesnick, J.; Lewis, C.; Mathieu, S.; Murray, J.; Nonomiya, J.; Pang, J.; Pegg, N.; Prior, W. W.; Rouge, L.; Salphati, L.; Sampath, D.; Tian, Q.; Tsui, V.; Wan, N. C.; Wang, S.; Wei, B.; Wiesmann, C.; Wu, P.; Zhu, B.-Y.; Olivero, A. *J. Med. Chem.* **2011**, *54*, 7579.
20. Castanedo, G.; Chan, B.; Lucas, M. C.; Safina, B.; Sutherlin, D. P.; Sweeney, Z. K. WO 2011101429 A1.
21. Goldsmith, P.; Hancox, T. C.; Hudson, A.; Pegg, N. A.; Kulagowski. J. J.; Nadin, A. J.; Price, S. WO 2009053716 A1.
22. Baker, S. J.; Goldsmith, P.; Hancox, T. C.; Pegg, N. A.; Price, S.; Shuttleworth, S. J. WO 2007122410 A1.
23. Griffen, E.; Leach, A. G.; Robb, G. R.; Warner, D. J. *J. Med. Chem.* **2011**, *54*, 7739.
24. The structure of compound **3** bound to (K802T) PI3Kγ has been deposited in the PDB under the code 4EZJ.
25. The structure of compounds **13** and **14** bound to (K802T) PI3Kγ have been deposited in the PDB under the codes 4EZK and 4EZL, respectively.
26. Kannan, N.; Neuwald, A. F. *J. Mol. Biol.* **2005**, *351*, 956.
27. Sutherlin, D. P.; Sampath, D.; Berry, M.; Castanedo, G.; Chang, Z.; Chuckowree, I.; Dotson, J.; Folkes, A.; Friedman, L.; Goldsmith, R.; Heffron, T.; Lee, L.; Lesnick, J.; Lewis, C.; Mathieu, S.; Nonomiya, J.; Olivero, A.; Pang, J.; Prior, W. W.; Salphati, L.; Sideris, S.; Tian, Q.; Tsui, V.; Wan, N. C.; Wang, S.; Wiesmann, C.; Wong, S.; Zhu, B.-Y. *J. Med. Chem.* **2010**, *53*, 1086.
28. Hall, S. W.; Cooke, A. *Mamm. Genome* **2011**, *22*, 377.
29. Compound **3** is a moderate time dependent inhibitor of CYP3A4 and was not pursued as a candidate for development. Efforts to limit this liability will be described elsewhere.
30. Obach, R. S.; Baxter, J. G.; Liston, T. E.; Silber, B. M.; Jones, B. C.; MacIntyre, F.; Rance, D. J.; Wastall, P. *J. Pharmacol. Exp. Ther.* **1997**, *283*, 46.